ELSEVIER

Chemical Engineering Journal 124 (2006) 19–28

Chemical Engineering Journal

www.elsevier.com/locate/cej

Methodology of multiphase reaction kinetics and hydrodynamics identification: Application to catalyzed nitrobenzene hydrogenation

Nader Frikha [a,*], Eric Schaer [b], Jean-Léon Houzelot [a]

[a] *Laboratoire des Sciences du Génie Chimique, CNRS, Ecole Nationale Supérieure des Industries Chimiques, INPL, 1 rue Grandville, BP 20451, 54001 NANCY Cedex, France*

[b] *Centre de Génie Chimique des Milieux Rhéologiquement Complexes, CNRS, Ecole Nationale Supérieure des Industries Chimiques, INPL, 1 rue Grandville, BP 20451, 54001 NANCY Cedex, France*

Received 24 April 2006; received in revised form 17 July 2006; accepted 7 August 2006

Abstract

This paper deals with the modelling of a multiphase batch reaction: catalyzed nitrobenzene hydrogenation. The reactor's gas–liquid mass transfer parameters in the absence of any reaction are first identified, and the solubility of hydrogen in the reactional medium is also measured. A reaction kinetics and heat parameter identification method is then developed. This method is based on a light experimental procedure, requiring measurement of only temperature and pressure variations in the batch reactor.

This study is carried out in an isothermal batch and semi-batch reactor, whose initial temperature varies between 283 and 333 K. A simplified model associating the hydrodynamic gas–liquid mass transfer parameters and the chemical kinetics processes is developed. The key parameters that can influence the reaction development are the hydrogen pressure, the coolant temperature, the quantity of catalyst pellets and the stirring speed. The developed model also allows the precise simulation of the extent of reaction and the temperature evolution of the studied multiphase catalytic reaction.

Keywords: Kinetics; Hydrodynamic; Multiphase reaction; Gas–liquid reaction modelling

1. Introduction

For several decades, a growing interest in the control of reactions carried out in discontinuous reactors has been observed. This type of reactor, characterized by a great flexibility, is much used in the pharmaceutical industry, fine chemistry and for the production of certain chemicals specialty (detergent, dye, perfumes, etc.) [1–3]. The majority of published studies devoted to batch reactors were developed for the control of homogeneous reactions, for which, most of the time, the studied parameters are the initial reactant concentrations and temperature. Fewer studies have been devoted to heterogeneous reactions in multiple phases [4,5], whose implementation is much more delicate [6]: contrary to homogeneous reactions, hydrodynamic parameters such as stirring speed, that can modify the multiphase mass transfer, should be taken into account.

This paper deals with the study, modelling and control of a batch heterogeneous reaction: the catalytic nitrobenzene hydrogenation reaction, using solid catalyst pellets containing palladium. This reaction obeys the following stoichiometry:

$$C_6H_5NO_2 + 3\,H_2 \rightarrow\ C_6H_5NH_2 + 2H_2O$$

The choice of this reaction allows for the illustration of two different points: first to study a kind of reaction which is widely used in fine chemistry and chemical specialities, and secondly, to illustrate the problems related to the thermal stability of batch or semi-batch heterogeneous reactors.

In the first section, the gas–liquid mass transfer parameters are measured in the absence of any reaction in the reactor, and the solubility of hydrogen in the reactional medium is also investigated. In the second section, a reaction kinetics and heat parameters identification method is proposed, and a model taking into account both the hydrodynamic and kinetic phenomena is developed.

* Corresponding author. Tel.: +33 3 83 17 50 88; fax: +33 3 83 17 50 86.
E-mail address: Nader.Frikha@ensic.inpl-nancy.fr (N. Frikha).

1385-8947/$ – see front matter © 2006 Elsevier B.V. All rights reserved.
doi:10.1016/j.cej.2006.08.012

Nomenclature

a	gas–liquid interfacial area (m^2)
A	heat transfer area (m^2)
A_p	particle geometric area (m^2)
C_a	Carberry number
C_{cat}	catalyst pellets concentration ($kg\,m^{-3}$)
C_{H_2}	concentration of hydrogen in the bulk liquid phase ($mol\,m^{-3}$)
$C^*_{H_2}$	interface hydrogen concentration on the liquid side in equilibrium with the gas ($mol\,m^{-3}$)
C_i	concentration of component i ($mol\,m^{-3}$)
C_p	specific heat capacity ($J\,kg^{-1}\,K^{-1}$)
D	diffusivity ($m^2\,s^{-1}$)
D_e	effective diffusivity ($m^2\,s^{-1}$)
E	activation energy ($J\,mol^{-1}$)
E_A	enhancement factor
F	flow ($mol\,s^{-1}$)
H_e	Henry constant for hydrogen ($Pa\,m^3\,mol^{-1}$)
k	rate constant ($m^{3(1+\alpha)}\,kg^{-1}\,s^{-1}\,mol^{-\alpha}$)
k'	rate constant ($m^3\,kg^{-1}\,s^{-1}$)
k_{app}	apparent kinetic constant (s^{-1})
k_L	gas–liquid mass transfer coefficient ($m^1\,s^{-1}$)
k_{LS}	liquid–solid mass transfer coefficient ($m^1\,s^{-1}$)
k_0	frequency factor ($m^{3(1+\alpha)}\,kg^{-1}\,s^{-1}\,mol^{-\alpha}$)
k'_0	frequency factor ($m^3\,kg^{-1}\,s^{-1}$)
m	mass (kg)
n_i	number of moles of component i (mol)
$n_{i,G}$	number of moles of component i in gaseous phase (mol)
N	stirrer speed (s^{-1} or rpm)
P	pressure (Pa)
P_v	vapour pressure (Pa)
Q	cumulated hydrogen consumption (m^3)
r	reaction rate ($mol\,m^{-3}\,s^{-1}$)
R	overall rate of hydrogenation ($mol\,m^{-3}\,s^{-1}$)
S	solubility ($mol\,m^{-3}$)
t	time (s)
T	temperature (K)
U	overall heat transfer coefficient ($W\,m^{-2}\,K^{-1}$)
V	volume (m^3)
V_{mol}	molar volume of hydrogen (NTP conditions) ($m^3\,mol^{-1}$)
x	mole fraction
X	conversion

Greek letters

$\Delta_r H$	enthalpy of reaction ($J\,mol^{-1}$)
$\Delta H_{vap,i}$	vaporization enthalpy of component i ($J\,mol^{-1}$)
ε_L	liquid holdup
ε_p	porosity of the catalyst particle ($kg\,m^{-3}$)
φ	thermal inertia
φ_t	Thiele modulus
ρ	density ($kg\,m^{-3}$)
τ	tortuosity of the catalyst pellets
Γ	molar heat capacity ($J\,mol^{-1}\,K^{-1}$)

Superscript

α	reaction order

Subscripts

amb	ambient
an	aniline
calc	calculated
cat	catalyst particle
exp	experimental
G	gas
L	liquid
nb	nitrobenzene
p	particle
w	wall
0	initial

2. Experimental setup

The reactor used in this study is a cylindrical stainless steel tank equipped with a jacket on its side wall. It was designed according to the traditional Holland and Chapman [7] configuration: the internal diameter is 0.11 m and the total volume is 1.39 l. Agitation is ensured by a Rushton turbine with right blades, whose stirring speed is controlled between 0 and 5000 rpm and a heating bath ensures the thermal regulation of the reactor. Several temperature probes (Pt 100), allow the tracking of the reactional medium and the external cooling liquid temperatures. The device is also equipped with a mass flow rate meter (Alborg 0–5 NL/min), that allows measurement of the instantaneous hydrogen consumption, and a pressure sensor (Keller, 0–5 bar). In order to ensure good bubble dispersion, the gas injection is performed through a plunging tube whose exit opening is placed right below the agitation mobile. A sketch of the experimental setup is presented in Fig. 1.

For each experiment 0.75 l of nitrobenzene (Prolabo Rectapur) are first loaded and mixed with the necessary quantity of catalyst pellets. The catalyst pellets consist of activated carbon particles, of 20 μm in size, filled with 5% by weight of palladium (Acros Organics). During and after the filling, a safety procedure has to be followed: the reactor is first purged using nitrogen and, by successive gas drainings, the gas phase is gradually replaced by pure hydrogen gas. The reaction begins when agitation is started. The temperature of the cooling liquid is controlled with a precision of ±0.1 K, and the reactor temperature, hydrogen pressure and hydrogen feed flow rate are recorded against time. The acquisition rate is 10 points/s. Since the minimal stirring speed for suspending the catalyst pellets, as determined using the relation of Joosten [6], is 810 rpm, it was decided that the minimal stirring speed should be 1000 rpm.

3. Measurements of mass transfer parameters

Before studying the reaction, the gas–liquid mass transfer coefficient (k_La) and solubility of hydrogen in the reactional medium were first measured.

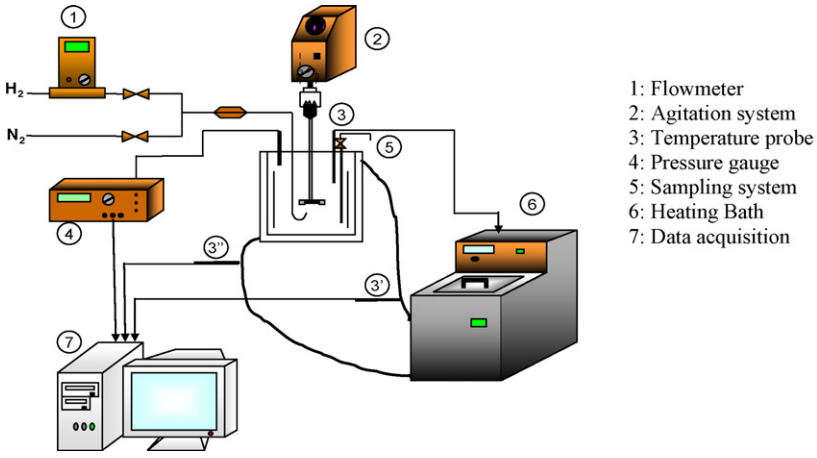

Fig. 1. Experimental setup.

Table 1
Compositions of various studied media

	S_1	S_2	S_3	S_4	S_5
x_{nb}	1.00	0.73	0.47	0.23	0.00
x_{an}	0.00	0.27	0.53	0.77	1.00

x_{nb} and x_{an} are respectively the nitrobenzene and aniline molar fractions.

3.1. Gas–liquid transfer coefficient k_La

3.1.1. Protocol and measurements

Determination of the gas–liquid transfer coefficient k_La has been realized using a physical absorption method based on pressure variation measurements and detailed in the following Refs. [8–11]. This method allows the simultaneous determination of the mass transfer coefficient k_La and of the gas solubility in the reactional medium.

The measurements were realized for several temperatures (T = 293, 313 and 333 K), several stirring speeds (between 1000 and 3000 rpm) and for several nitrobenzene–aniline mixtures in order to take into account the influence of reactional composition, which changes gradually from pure nitrobenzene to aniline as the reaction proceeds. The compositions of the various media studied are presented in Table 1.

A statistical processing of the gas–liquid mass transfer coefficient k_La measurements (Student's test with an accuracy of 95%) showed that the results can be estimated with an uncertainty of approximately 4.2%, which is satisfactory for these kinds of measurements. The variations of k_La against stirring speed and temperature for pure nitrobenzene and aniline are presented in Fig. 2.

3.1.2. Influence of stirring speed and temperature

As expected, the values of k_La increase with the stirring speed. The increase of temperature also slightly accelerates the gas to liquid mass transfer. Indeed, the temperature has two combined effects: for high temperature values, surface tension, density and viscosity decrease, which induces the formation of smaller bubbles and thus increases the interfacial area a [10,12]. Moreover, the increase in diffusivity also induces an increase in the mass transfer coefficient k_L.

A semi-empirical law that describes the variations of the hydrogen gas–liquid transfer coefficient k_La with stirring speed and temperature, respectively, in nitrobenzene and aniline, can then be proposed:

$$k_La_{nb} = 4.17 \times 10^{-12} T^{2.52} N^{3.1} \quad \text{and}$$
$$k_La_{an} = 2.77 \times 10^{-12} T^{2.52} N^{3.1} \qquad (1)$$

The variations of k_La for different reactional media (S_1, S_2, S_3, S_4 and S_5) and a temperature of 313 K are presented in Fig. 3. The experimental values for varying compositions can be fit by

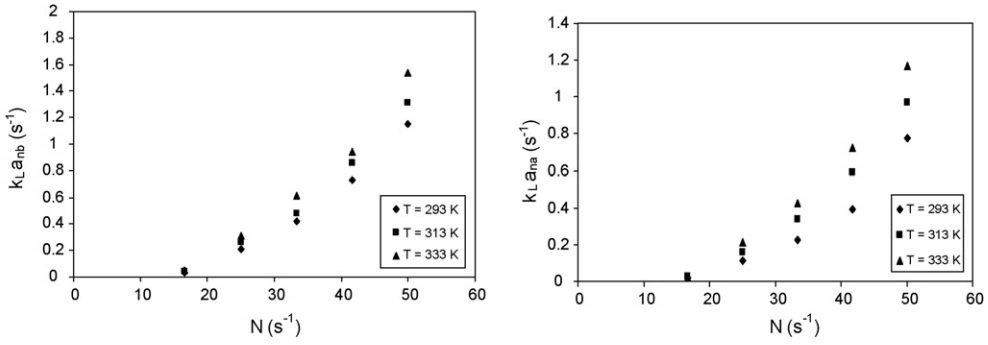

Fig. 2. Effect of the temperature and stirring speed on the hydrogen in nitrobenzene and aniline (S_1 and S_5) mass transfer coefficient.

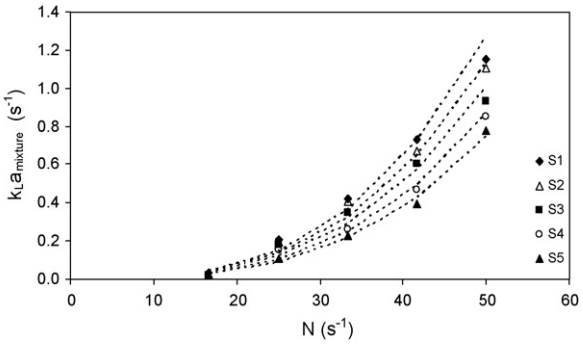

Fig. 3. Mass transfer coefficients for various media against temperature and stirring speed, $T = 313$ K.

the following correlation, plotted in dotted line in Fig. 3:

$$k_L a_{mixture} = x_{nb} k_L a_{nb} + x_{an} k_L a_{an} \quad (2)$$

3.1.3. Influence of the quantity of solid particles

Several studies dealing with the influence of solid particles on the mass transfer coefficient k_La have been carried out [8,11,13,14]. It remains difficult however to propose a general relation describing the variation of the mass transfer coefficient k_La with the quantity of solid particles, whatever their material may be.

A series of experimental measurements are shown here: in the case of activated carbon particles of 20 μm in average size and for concentrations ranging between 0 and 2 kg/m^3, the influence of solid on the measured transfer coefficient is negligible, as can be seen in Fig. 4, describing the variations of the measured transfer coefficient with stirring speed for different solid concentrations.

3.2. Solubility

3.2.1. Protocol and measurements

The determination of hydrogen solubility, or Henry coefficient, was performed according to the following procedure. After equilibrating hydrogen and solvent under the pressure, P_i, agitation was stopped and the pressure of hydrogen within the reactor was quickly increased at P_0. Agitation was started again, until reaching another equilibrium state (P_f). A mass balance between

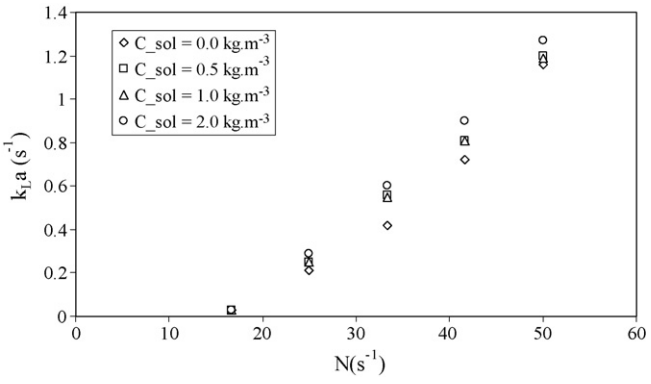

Fig. 4. Mass transfer coefficient against stirring speed for different solid concentrations, $T = 313$ K.

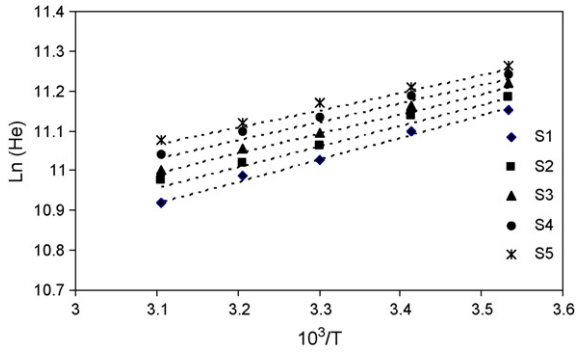

Fig. 5. Henry coefficient against reciprocal temperature.

the two equilibrium states leads to [8]:

$$H_e = \frac{V_L RT}{V_G} \frac{P_f - P_i}{P_0 - P_f} \text{ (Pa mol}^{-1}\text{ m}^3\text{)} \quad (3)$$

The relation between the Henry coefficient and solubility can be expressed as follows:

$$C^*_{H_2} = \frac{P_{H_2}}{H_{e,H_2}} \text{ (mol m}^{-3}\text{)} \quad (4)$$

Measurements were realized for temperatures ranging between 283 and 323 K, and a reproducibility test showed that the error of measurement was about 3%.

Hydrogen Henry coefficients for the pure nitrobenzene and aniline are, respectively:

$$H_{e,nb}(T) = 1.00 \times 10^4 \exp\left(\frac{551}{T}\right) \text{ (Pa m}^3\text{ mol}^{-1}\text{)} \quad (5)$$

$$H_{e,an}(T) = 1.66 \times 10^4 \exp\left(\frac{439}{T}\right) \text{ (Pa m}^3\text{ mol}^{-1}\text{)} \quad (6)$$

3.2.2. Influence of liquid composition

For ideal mixtures, Hichri [15] proposed the use of the following empirical relation:

$$\ln(H_{e,mixture}) = x_1 \ln(H_{e,1}) + x_2 \ln(H_{e,2}) \quad (7)$$

When applied to the experimental measurements realized for different nitrobenzene and aniline compositions, this relation (only valid for an ideal mixture) has good agreement, as can be seen in Fig. 5, where the dotted line corresponds to relation (7).

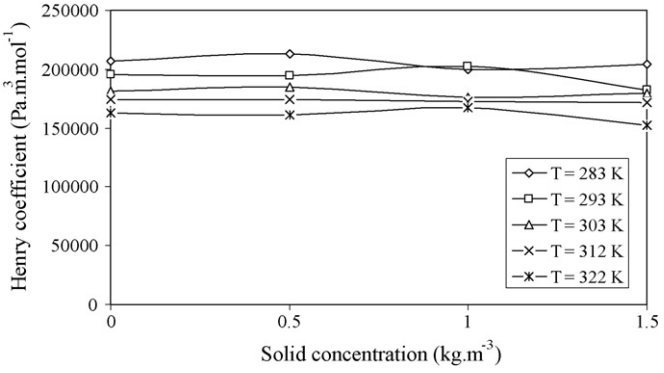

Fig. 6. Henry coefficient against solid concentration.

Finally it has been also experimentally shown that solid particles do not have a significant influence on the solubility of hydrogen in nitrobenzene or aniline, as can be seen in Fig. 6, describing the variations of hydrogen solubility in nitrobenzene against solid concentrations for different temperatures.

4. Measurement of the reaction kinetics

4.1. Protocol

The objective was here to determine an apparent kinetic law for the catalyzed nitrobenzene hydrogenation using a light experimental procedure. The measurements were carried out in batch mode for the liquid and gas phases according to the following protocol: once the reactional mixture has been loaded and hydrogen drainings carried out, the reactor is pressurised under 3×10^5 Pa. As soon as agitation is started up, a pressure decrease is observed, while the reactional temperature remains unchanged. The experiment is stopped when all hydrogen has been consumed ($P_{H_2} \approx 0$).

In order to assure isothermal conditions, the cooling bath temperature was regulated according to the reactor temperature, and the cooling liquid temperature varied in order to keep a constant reactional temperature.

The advantage of such a methodology is that experiments are carried out with a very high under-stoichiometry of hydrogen compared to that of nitrobenzene (of about 1 per 1000), so that for each experiment, the nitrobenzene conversion remains very low. Thus, multiple experiments can be carried out with the same reactional medium with neither draining nor renewal.

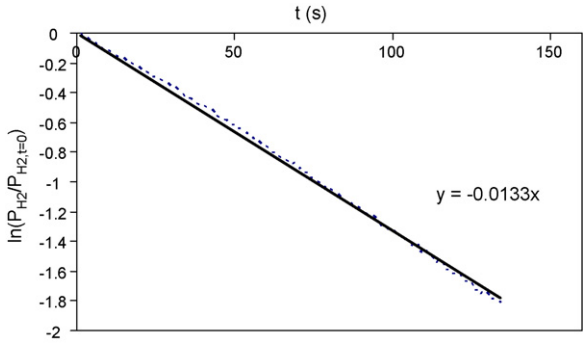

Fig. 7. Determination of k_{app}: $C_{cat} = 1\ kg\ m^{-3}$, $N = 3000$ rpm, $T = 303$ K.

4.2. Determination of the apparent kinetics rate

For each run, it can be shown that the pressure drop against time follows a decreasing exponential law, which is characteristic of an apparent first-order kinetic reaction in hydrogen.

A global mass balance on the gas phase during the batch experiment leads to:

$$-\frac{dn_{H_2}}{dt} = -\frac{V_G}{RT}\frac{dP_{H_2}}{dt} = k_{app}\frac{V_G}{RT}P_{H_2} \quad (8)$$

$$\frac{dP_{H_2}}{dt} = -k_{app}P_{H_2} \quad \text{and then} \quad \ln\left[\frac{P_{H_2}}{P_{H_2,t=0}}\right] = -k_{app}t \quad (9)$$

As an example, the variation of hydrogen pressure is presented on a logarithmic scale for a typical experiment in Fig. 7. A straight line of slope $-k_{app}$ is obtained, consistent with an

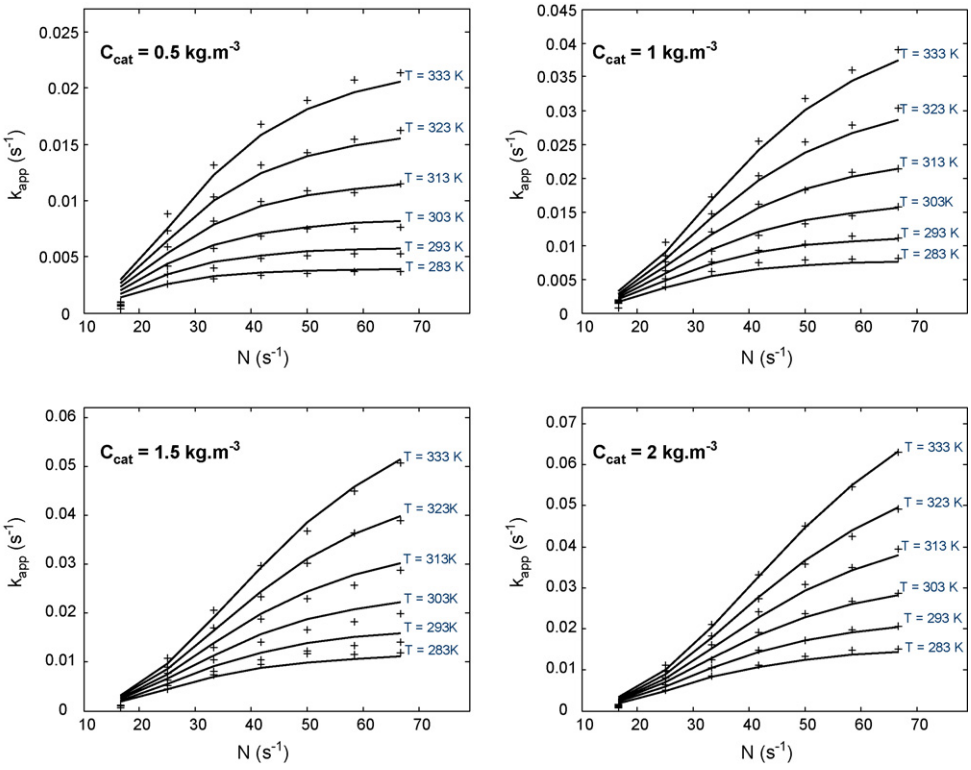

Fig. 8. Variation of k_{app} against stirring speed, temperature and pellet concentration.

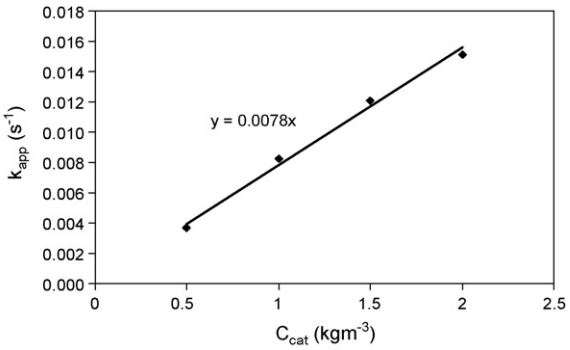

Fig. 9. Variation of the apparent kinetics constant against pellet concentration, $T = 283$ K, $N = 4000$ rpm.

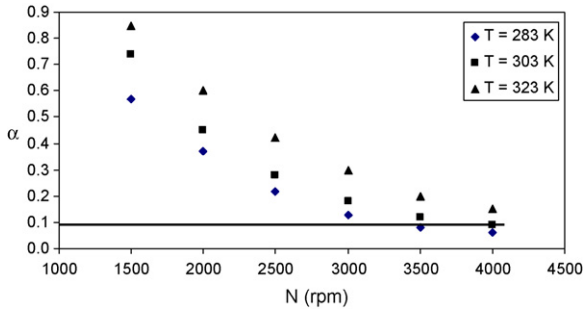

Fig. 10. Gas–liquid mass transfer limitations, $C_{cat} = 1\ kg\ m^{-3}$.

apparent first-order reaction in hydrogen. The experimental error is about 3.5%.

Four series of experiments were carried out for varying catalyst pellet concentrations in the range 0.5–2 kg/m^3. The choice of this concentration level was based on former studies on hydrogenation reactions in organic mediums [16–18]. For each series, the temperature ranged between 283 and 333 K with steps of 10 K and, for each temperature, the stirring speed increased from 1000 to 4000 rpm with steps of 500 rpm. Fig. 8 presents all the measured values of k_{app}.

The experimental values of k_{app} increase with stirring speed and temperature. This observation shows that both the mass transfer in the liquid boundary layer and the reaction kinetics, which are activated by temperature rise, have an influence on the apparent kinetic rate. For the lowest temperatures and highest stirring speeds, the values of k_{app} become almost constant. Theses threshold values show that the reaction then proceeds in a reaction-rate limited mode or chemical regime, characteristic of the absence of any hydrodynamic or diffusional limitations.

These threshold values allow for the determination of the chemical reaction kinetics in the absence of any limitations. Indeed, the proportionality between such determined apparent kinetic rates and catalyst concentrations, as can be seen in Fig. 9, suggests the absence of any mass transfer limitation.

4.3. Mass transfer limitations

For a heterogeneous gas–liquid–solid batch catalysed reaction, mass transfer first takes place from the gas phase to the liquid phase, then from the bulk fluid to the external surface of the pellet and finally, reactants diffuse through the pellets, where reaction takes place on the catalytic surface. Several mass transfer limitations (gas–liquid, liquid–solid and internal diffusion) should be taken into account, and the development of a complete kinetic model requires the determination of the limiting regimes.

4.3.1. Gas–liquid mass transfer

Mills [5] and Rode [17] have defined an adimensional number, α which represents the ratio of the observed hydrogen consumption rate to the gas dissolution rate in the pure liquid phase:

$$\alpha = \frac{R_{H_2}}{k_L a C^*_{H_2}} \tag{10}$$

In absence of any gas–liquid mass transfer limitations, the adimensional number, α must be lower than 0.1.

Since the observed consumption rates, R_{H_2}, vary against time, their initial and highest values, corresponding to the situation where the gas–liquid limitations are the most significant, have been chosen for the estimation of α.

For high stirring speeds and for low catalyst pellet concentrations or temperatures, the values of α are lower than 0.1, which is characteristic of the absence of any gas–liquid transfer limitation. However, all other process conditions lead to values higher than 0.1, as can be seen in Fig. 10 for a catalyst pellet concentration of 1 kg m^{-3} and for various stirring speeds and temperatures.

The gas–liquid mass transfer limitations are thus significant, and should be taken into account in the mathematical description of the reaction.

4.3.2. Liquid–solid mass transfer

The Carberry number, Ca, allows for the estimation of the limitations of the transfer from the bulk fluid to the external surface of the pellet, also described as external mass transfer:

$$Ca = \frac{R_{H_2}}{k_{LS} C_{cat} C_{H_2} A_p / V_p \rho_p} \tag{11}$$

The external mass transfer limitation is negligible when $Ca < 0.1$ [19].

The liquid–solid mass transfer coefficient (k_{LS}), was estimated according to the correlation of Armenante and Kirwan [20] which seems appropriate, given the size of the catalyst pellets. The concentration of hydrogen in the bulk liquid phase can be related to the overall hydrogenation rate and the mass transfer coefficient as (see section 4.4 and Fig. 13):

$$R_{H_2} = k_L a (C^*_{H_2} - C_{H_2}) \quad \text{so that} \quad C_{H_2} = C^*_{H_2} - \frac{R_{H_2}}{k_L a} \tag{12}$$

When the mass transfer coefficient is larger than the overall hydrogenation rate, the Carberry number can thus be evaluated using the hydrogen solubility.

Fig. 11 presents the variations of the Carberry number for a catalyst pellet concentration of 1 kg m^{-3} and for various stirring

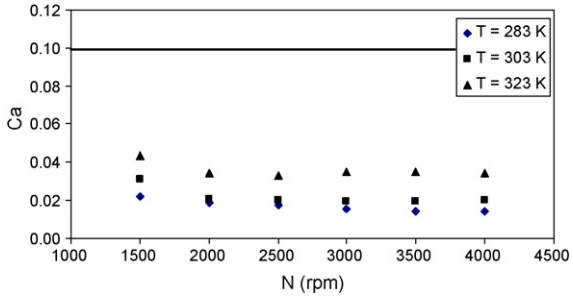

Fig. 11. Liquid–solid mass transfer limitations, $C_{cat} = 1\ kg\ m^{-3}$.

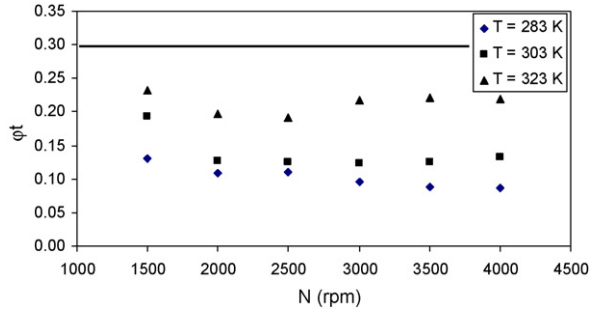

Fig. 12. Internal mass transfer limitations, $C_{cat} = 1\ kg\ m^{-3}$.

speeds and temperatures. All calculated values of *Ca* remain far lower than 0.1, supporting the hypothesis that there are no liquid–solid transfer limitations. The external mass transfer is thus not significant and will be neglected in the developed model.

4.3.3. Internal diffusion mass transfer

The calculation of the Thiele modulus allows for the determination of the influence of the internal diffusional limitation into the pellets. For $\varphi_t < 0.3$ the internal diffusion limitation is negligible:

$$\varphi_t = \left(\frac{R_{H_2}}{D_{eff} C_{cat} C_{H_2} / L_p^2 \rho_p} \right)^{1/2} \tag{13}$$

with D_{eff} the effective diffusivity $D_{eff} = \varepsilon_p D/\tau$.

The tortuosity depends on the porosity, and has been calculated according to the relation of Lordgooei et al. [21]. The hydrogen in nitrobenzene diffusion coefficient was estimated using the Wilke and Chang [22], Tyn and Callus [23] and Nakanishi [24] correlations, which all lead to similar values. The characteristic data of the catalyst pellets are gathered in Table 2. Finally, the hydrogen concentrations were estimated using relation (12).

The variations of the Thiele modulus for a catalyst pellet concentration of $1\ kg\ m^{-3}$ and different stirring speeds or temperatures are presented in Fig. 12. The values of φ_t are between 0 and 0.27 and remain, for varying operating conditions, smaller 0.3.

Thus, the internal diffusion mass transfer limitations will not be taken into account in the proposed model.

4.4. Development of a global model, determination of the kinetic parameters

The preceding paragraphs have shown that only gas–liquid mass transfer limitations should be taken into account to describe the batch catalysed nitrobenzene hydrogenation reaction.

Table 2
Characteristic data of the catalyst pellets

Specific surface area	$1000\ m^2\ g^{-1}$
Porosity	0.53
Tortuosity	2
Diffusion coefficient (calculated)	$2.88 \times 10^{-9}\ m^2\ s^{-1}$
Apparent density	$530\ kg\ m^{-3}$
Particle mean size	<20 μm

A mass balance on hydrogen consumption gives:

$$-\frac{dn_{H_2}}{dt} = -\frac{V_G}{RT}\frac{dP_{H_2}}{dt} = \frac{V_G}{RT} k_{app} P_{H_2}$$
$$= V_L k_L a E_A \left(\frac{P_{H_2}}{H_e} - C_{H_2} \right) = V_L k' C_{cat} C_{H_2} \tag{14}$$

The last term on the right-hand side corresponds to the chemical consumption of hydrogen. The apparent first-order reaction in hydrogen has already been observed for all the performed experiments, and as nitrobenzene conversion remains very low during an experiment, the nitrobenzene concentration is supposed to remain as constant.

After reorganization, relation (14) gives:

$$\frac{V_L RT}{V_G H_e} \frac{1}{k_{app}} = \frac{1}{k'_{app}} = \frac{1}{k_L a E_A} + \frac{1}{k' C_{cat}} \tag{15}$$

To use relation (15), it is necessary to estimate the value of the enhancement factor E_A. When comparing the hydrogen consumption rates in the absence (absorption alone) and presence (absorption and reaction) of catalyst pellets, for the same operating conditions (Fig. 13), it can be remarked that these two rates are identical, even if physical absorption ends up much earlier than adsorption with reaction. This remark, which applies to all the performed experiments means that the reaction does not accelerate the mass transfer whatever the values of the process parameters, and that the enhancement factor can be considered to be equal to 1.

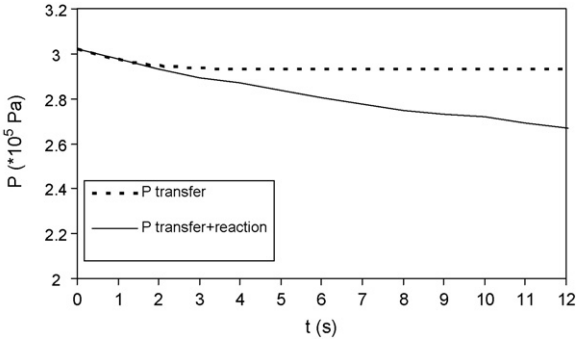

Fig. 13. Comparison between initial hydrogen in nitrobenzene consumption rates, $N = 3000$ rpm, $C_{cat} = 0.5\ kg\ m^{-3}$, $T = 293$ K.

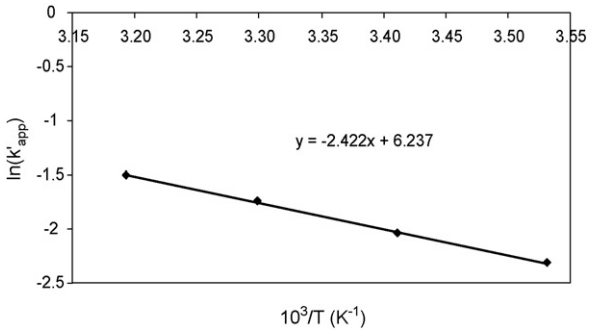

Fig. 14. Determination of activation energy, $C_{cat} = 0.5\,kg\,m^{-3}$.

Finally, relation (15) can be rewritten as

$$\frac{1}{k'_{app}} = \frac{V_L RT}{V_G H_e}\frac{1}{k_{app}} = \frac{1}{k_L a} + \frac{1}{k' C_{cat}} \tag{16}$$

The more significant agitation is, the more the transfer coefficient value, $k_L a$, is high, and the more the term $1/k_L a$ becomes negligible compared to $1/k' C_{cat}$. Under these conditions, $k'_{app,lim}$ is the limiting value of k'_{app} for the highest stirring speeds.

Since $k'_{app,lim}$ corresponds to the reaction rate limited mode, in the absence of any mass transfer limitation, their values can be used to measure the apparent activation energy and frequency factor of the catalysed nitrobenzene hydrogenation. The following relation can be written:

$$k'_{app,lim} = k' C_{cat} = k'_0 \exp\left(-\frac{E}{RT}\right) C_{cat} \tag{17}$$

Thus plotting $k'_{app,lim}$in an Arrhenius diagram (Fig. 14) gives

$$\frac{E}{R} = 2422\,K \quad (E = 20.14\,kJ\,mol^{-1}) \quad \text{and}$$

$$k'_0 = 1023\,(m^3\,kg^{-1}\,s^{-1})$$

The activation energy value determined in this study is close to the value reported by Acres and Cooper [18]: $E = 23.2\,kJ\,mol^{-1}$. The hydrogen consumption rates measured here are also of the same order of magnitude as those reported by the same authors [18], for high nitrobenzene concentrations.

Finally, taking the numerical expression determined by the physical procedure (relations (1) and (2)) for $k_L a$, the values of the apparent constant, k_{app}, can be re-calculated, and are superimposed (in a continuous line) with the experimental measurements in Fig. 8. It can be remarked that the agreement is satisfactory.

4.5. Reaction in semi-batch mode

4.5.1. Introduction

The objective of this part was to carry out the reaction until total conversion of nitrobenzene was achieved. The experimental procedure remained practically identical to that described previously, except that the pressure was kept constant. For these experiments, as soon as agitation begins, the reaction starts and hydrogen consumption is followed by a mass flow rate meter. Thus, at every moment, if the accumulation terms are neglected, the measurement of the instantaneous hydrogen flow rate allows for the estimation of the rate of nitrobenzene consumption. Finally, as the heat released by the reaction is now more significant (since nitrobenzene conversion is increased), the reactor is no longer supposed as isothermal, and the experiments are carried out in isoperibolic mode.

The interpretation of such experiments requires the development of a model which takes into account mass and heat balances in the reactor, and developed according to the following assumptions:

- The gas phase is supposed to be composed of hydrogen and vapour of various reactants and products appearing or disappearing as the reaction proceeds.
- The variation of the organic phase reactional volume during an experiment is taken into account. The variations of solubility and diffusivity of hydrogen against temperature are also described. The water produced during the reaction is supposed as being insoluble in the organic phase, and the solubilities of nitrobenzene and aniline in aqueous phase are also neglected [25].

4.5.2. Mass balance

The cumulative hydrogen flow rate allows for the definition of a nitrobenzene conversion extent as:

$$X(t) = \frac{Q_{H_2}(t)}{3 V_{mol} n_{nb,0}} \tag{18}$$

Taking the same expressions as those developed for experiments performed in batch mode, the mass balance is written:

$$F_{H_2}(t) = r_{H_2} V_L = k_{app}\frac{V_G}{RT} P_{H_2} = k_L a V_L (C^*_{H_2} - C_{H_2}) = k C_{H_2} C_{cat} C^{\alpha}_{nb} V_L \tag{19}$$

with

$$k = k_0 \exp\left(-\frac{E}{RT}\right) = \frac{k'}{C^{\alpha}_{nb}} = \frac{1}{C^{\alpha}_{nb}} k'_0 \exp\left(-\frac{E}{RT}\right).$$

This expression allows for the definition of a nitrobenzene reaction rate and the variation of the nitrobenzene reaction extent against reaction time:

$$r_{nb} = \frac{r_{H_2}}{3} = \frac{1}{3}\frac{P_{H_2}(t)/H_e}{(1/(k_0\ \exp(-E/RT) C_{cat} C^{\alpha}_{nb})) + (1/k_L a)} \quad \text{and}$$

$$\frac{dX}{dt} = \frac{1}{3 C_{nb,0}} \times \frac{P_{H_2}(t)/H_e}{(1/(k_0 \exp(-E/RT) C_{cat} C^{\alpha}_{nb,0}(1-X)^{\alpha})) + (1/k_L a)} \tag{20}$$

4.5.3. Heat balance

The heat balance can be written as

$$UA(T_w - T) = m C_P \varphi \frac{dT}{dt} + V_L r_{nb} \Delta_r H + F_{H_2} \Gamma_{p,H_2} (T - T_{amb}) + \frac{dn_{nb,G}}{dt}\Delta H_{vap,nb} + \frac{dn_{an,G}}{dt}\Delta H_{vap,an} + \frac{dn_{H_2O,G}}{dt}\Delta H_{vap,H_2O} \tag{21}$$

Table 3
Semi-batch experiments conditions and parameters

	1	2	3	4	5	6	7	8	9	10	11	12	13
N (rpm)	2500	2500	2500	2500	1200	1500	2000	3000	1200	1500	2000	3000	3000
C_{cat} (kg m^{-3})	0.5	1	1.5	2	1	1	1	1	1.5	1.5	1.5	1.5	0.5

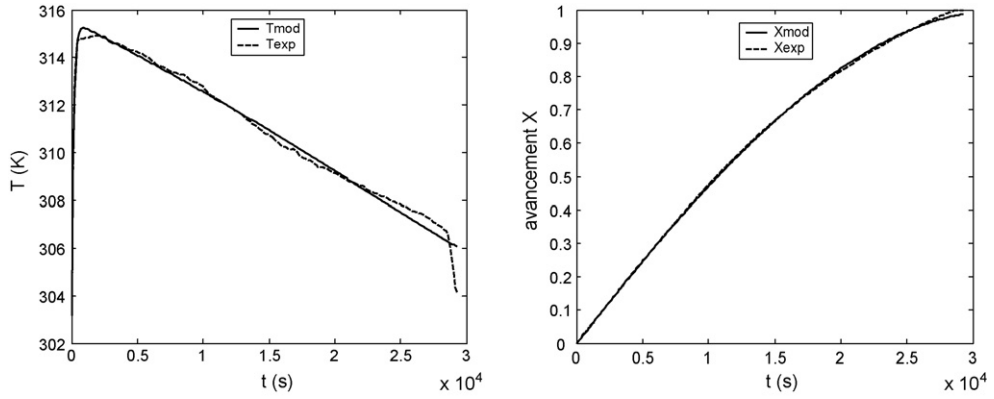

Fig. 15. Example of the comparison between the experimental and modelled temperature and conversion profiles, $N = 2000$ rpm, $C_{cat} = 1.5\,kg\,m^{-3}$, $P = 3 \times 10^5$ Pa, $T_w = 303$ K.

This balance takes into account the heating of the hydrogen flow into the system as well as the vaporization enthalpy of the water, nitrobenzene and aniline.

The overall heat transfer coefficient UA and the thermal inertia φ have been obtained following an experimental calorimetric study. The procedure consists of the heating of the reactor containing reactants (without catalyst pellets) by a thermal source of known power and to follow the temperature evolution against time. The resolution of the heat balance in such conditions leads to a thermal inertia φ of 1.125 and an overall heat transfer coefficient UA of 14.1 W K^{-1}.

The gas phase composition is defined using the liquid vapour equilibrium relations. The device allows for the maintenance of the gas phase pressure at a constant value P_t. Thus, at every moment:

$$P_{H_2}(t) = P_T - P_{nb}(T) - P_{an}(T) - P_{H_2O}(T) \quad (22)$$

where $P_{nb}(T)$, $P_{an}(T)$ and $P_{H_2O}(T)$ represent respectively the partial pressures of nitrobenzene, aniline and steam at the temperature $T(t)$.

Based on the assumption of the liquid phase composition detailed above, it is supposed that the partial pressure of water is equal to its saturating vapour tension at the considered temperature, and that the aniline–nitrobenzene mixture is ideal. As follows:

$$P_{H_2O}(T) = P_{v,H_2O}, \qquad P_{nb}(T) = x_{nb} P_{v,nb},$$
$$P_{an}(T) = (1 - x_{nb}) P_{v,an} \quad (23)$$

where x_{nb} represents the molar ratio of nitrobenzene in the organic phase and $P_{v,nb}$, $P_{v,an}$, P_{v,H_2O}, are the saturating vapour pressures of nitrobenzene, aniline and water.

In this approach, one should not lose sight of the fact that the boiling points of nitrobenzene and aniline are much higher than that of water and thus, that it is the evaporation of water, in particular, which has to be taken into account in the heat balance.

By identifying this model in a series of semi-batch experiments whose conditions are gathered in Table 3, we could identify and validate the model by a simultaneous nonlinear regression based on the profiles of conversion and temperature against time. Fig. 15 shows, for a particular case, that the agreement is satisfactory.

This developed model allows for a better specification of the chemical kinetics law. The reaction order in nitrobenzene was found to be 1/3, and the chemical reaction rate per mole of hydrogen can finally be expressed as:

$$r_{H_2} = 47.8 \exp\left(-\frac{2422}{T}\right) C_{cat} C_{nb}^{1/3} C_{H_2} \,(\text{mol m}^{-3}\,\text{s}^{-1}) \quad (24)$$

5. Conclusion

Initially, a study of the gas–liquid mass transfer was performed to determine the global mass transfer coefficient, $k_L a$, and the solubility of hydrogen in the reactional medium. We have shown that the mass transfer coefficient varies with the stirring speed at the order 3.1, and is thus proportional to the dissipated power in the vessel. The influence of solid particles on the transfer coefficient, $k_L a$, and solubility proved to be negligible for the studied concentrations.

A reaction kinetics and heat parameters identification method, based on temperature and pressure measurements within the reactor, was then developed and applied to batch experiments. The apparent kinetics of the catalysed nitrobenzene hydrogenation was deduced by pressure variations over time. If batch reactors are sometimes difficult to analyse, from the numerical resolution point of view, such reactors allow for the performance of kinetics measurements in a simple and fast

way. Indeed, the advantage of such a methodology, using a very high under-stoichiometry of gas, is to allow for great number of experiments, without renewing the liquid reactant.

Finally a complete kinetic study, based on the resolution of heat and mass balances in semi-batch mode, was carried out to precisely identify the reaction kinetics and to develop a model associating the gas liquid mass transfer and chemical kinetics processes.

This reaction, of easy implementation and whose kinetics rate can be varied according to the catalyst pellets quantity, can further be used as a model reaction for the study of thermal stability or thermal runaways of heterogeneous batch and semi-batch reactors.

References

[1] N. Aziz, I.M. Mujtaba, Chem. Eng. J. 85 (2002) 313–325.
[2] M.P. Dudukovic, F. Larachi, P.L. Mills, Chem. Eng. Sci. 54 (1999) 1975–1995.
[3] M. Soroush, C. Kravaris, Ind. Eng. Chem. Res. 32 (1993) 866–881.
[4] P.O. Mchedlov-Petrossyan, W.B. Zimmerman, G.A. Khomenko, Chem. Eng. Sci. 58 (2003) 2691–2703.
[5] P.L. Mills, R.V. Chaudhari, Catal. Today 37 (1997) 367–404.
[6] G.E.H. Joosten, J.G.M. Schilder, A.M. Broere, Trans IchemE 55 (1977) 220–222.
[7] F.A. Holland, F.S. Chapman, Liquid Mixing and Processing in Stirred Tanks, Reinhold Publishing Corporation, 1966, pp. 12–13.
[8] E. Dietrich, C. Mathieu, H. Delmas, J. Jenck, Chem. Eng. Sci. 47 (1992) 3597–3604.
[9] R.V. Chaudhari, R.V. Gholap, G. Emig, H. Hofman, Can. J. Chem. Eng. 65 (1987) 744–751.
[10] E. Crezee, B.W. Hoffer, R.J. Berger, M. Makkee, F. Kapteijn, J.A. Moulijn, Appl. Catal. 251 (2003) 1–17.
[11] B.W. Hoffer, P.H.J. Schoenmakers, P.R.M. Mooijman, G.M. Hamminga, R.J. Berger, A.D. van Langeveld, J.A. Moulijn, Chem. Eng. Sci. 59 (2004) 258–269.
[12] G.E.H. Joosten, J.G.M. Schilder, J.J. Janssen, Chem. Eng. Sci. 32 (1977) 563–566.
[13] C. Joly-Vuillemin, C. de Bellefon, H. Delmas, Chem. Eng. Sci. 51 (1996) 2149–2158.
[14] A.A.C.M. Beenackers, W.P.M. Van Swaaij, Chem. Eng. Sci. 48 (1993) 3109–3139.
[15] H. Hichri, A. Accary, J.P. Puaux, J. Andrieu, Ind. Eng. Chem. Res. 31 (1992) 1864–1867.
[16] C.V. Rode, M.J. Vaidya, R. Jaganathan, R.V. Chaudhari, Chem. Eng. Sci. 56 (2001) 1299–1304.
[17] C.V. Rode, R.V. Chaudhari, Ind. Eng. Chem. Res. 33 (1994) 1645–1653.
[18] G.J.K. Acres, B.J. Cooper, J. Appl. Chem. Biotechnol. 22 (1972) 769–785.
[19] S.P. Lee, Y.W. Chen, J. Mol. Catal. A: Chem. 152 (2000) 213–223.
[20] P.M. Armenante, D.J. Kirwan, Chem. Eng. Sci. 44 (1989) 2781–2796.
[21] M. Lordgooei, M.J. Rood, M. Rostom-Abadi, Environ. Sci. Technol. 35 (2001) 613–619.
[22] C.R. Wilke, P. Chang, AICHE J. 1 (1955) 264–270.
[23] M.T. Tyn, W.F. Calus, J. Chem. Eng. Data 20 (1975) 106–109.
[24] K. Nakanishi, Ind. Eng. Chem. Fundam. 17 (1978) 253–256.
[25] J.C. Smith, N.J. Foecking, W.P. Barber, Ind. Eng. Chem. 41 (1949) 2289–2291.